International Journal of Innovative
Computing, Information and Control
Volume **14**, Number **6**, December **2018**

ICIC International ©2018 ISSN 1349-4198
pp. 2163–2174

SLIDING MODE CONTROL WITH RBFNN COMPENSATION FOR DYNAMIC POSITIONING OF SHIP WITH DISTURBANCES AND INPUT SATURATION

Guoqing Xia[1], Jingjing Xue[1,*], Chuang Sun[1] and Ying Yang[2]

[1]College of Automation
Harbin Engineering University
No. 145, Nantong Street, Nangang District, Harbin 150001, P. R. China
{ xiaguoqing; sunchuang }@hrbeu.edu.cn; *Corresponding author: xuejingjing@hrbeu.edu.cn

[2]Marine Design and Research Institute of China
China State Shipbuilding Corporation
No. 1688, Xizang South Road, Shanghai 200011, P. R. China

Received January 2018; revised May 2018

Abstract. *This paper proposed a sliding mode controller with radial basis function neural network (RBFNN) compensation for dynamic positioning (DP) ships to steer ship to desired position under the problems of external environmental disturbances and input saturation. Using RBFNN to compensate the uncertainties in input saturation, the sliding mode control (SMC) law is designed under the disturbances, and then, the stability of the designed control law is proved uniform asymptotic stability on the basis of Laypunov stability theory. To validate the performance of designed control scheme, three groups of simulation results of the proposed control law compared to proportion integration differentiation (PID) control law are demonstrated to verify the effectiveness of the proposed control law.*

Keywords: Sliding mode control, RBF neural network, Dynamic positioning, Input saturation

1. **Introduction.** DP is defined as only depending on actuators to automatically keep its fixed location or predetermined track [1]. And in DP control system, problems such as complex nonlinearities, input saturation, unmodelled dynamics, external disturbances, and parameter uncertainties are commonly challenges appearing in controller designed process. To deal with these problems, DP control system has experienced several stages, from PID control, advanced output feedback control, to nonlinear adaptive control and hybrid intelligent control, improving the performance and maneuverability of ships with DP control system. And mixing two or more control methods such as backstepping technique, SMC, fuzzy control, model predictive control, PID control, and adaptive control is common control scheme to solve problems in DP control system [1-8].

In these control methods, sliding mode control (SMC) caught the researchers' eyes because of strong robustness for its invariance to system uncertainties and external disturbances [9-11]. Adaptive SMC of multi-input multi-output (MIMO) nonlinear controller was designed to deal with uncertainties in [9] and verified by simulations of a two-link manipulator. Similarly, [10] proposed a new adaptive SMC scheme using integral/exponential adaptation law to improve slow response and gain overestimation for MIMO nonlinear systems with uncertainties and unknown bounds available inputs. And the problem of input saturation has attracted a lot of researchers' interest [4,14-17]. Due to the limiting of

DOI: 10.24507/ijicic.14.06.2163

actuators such as thrusters, and propellers, the input saturation phenomenon commonly exists in DP control system, which affects the stabilization and performance of control system or leads to system instability. This increases difficulty to analyze and design controller. Combining disturbance observer with an auxiliary dynamic system, [4] utilized dynamic surface control technique to handle input saturation and disturbances. The tracking error dynamic system was divided into two subsystems and the subsystems used backstepping technique separately to cope with input saturation in global tracking control system in [18]. Besides, due to preferable approach ability of RBFNN, combining SMC with RBFNN is one of available methods to handle with uncertainties and disturbances in control system, especially in problem of input saturation [12-15]. The uncertainties were estimated and compensated by RBFNN in path following control of unmanned marine surface vessel and the input saturation phenomenon was solved by using backstepping technique [13]. However, rarely few papers used RBFNN compensation to solve the uncertainties of control forces and moment in input saturation for DP control system. And in real DP control system, model uncertainties and input saturation phenomenon exist and affect the stabilization and performance of control system or lead to system instability. Therefore, the motivation of this paper is to combine the approaching ability of RBFNN with the invariance to system uncertainties of SMC method in order to deal with problems of input saturation and uncertainties in DP control system. Thus, the main contribution of this paper is to develop a control scheme combining RBFNN with SMC to solve problems of environmental disturbances and input saturation. Specifically, this scheme is to design SMC law based on Laypunov stability theory utilizing RBFNN compensation to offset uncertainties in input forces and moment, and compare the designed control law to PID control law with three groups of simulation results in order to intuitively present the advantages and disadvantages of the two methods for DP control system.

The structure of this paper is organized as follows. Section 2 states the control problem of DP ships subject to uncertain disturbances and input saturation. Section 3 presents the design of sliding mode control by using RBFNN. The stability of designed control law is also proved in this section. Simulation results and discussions without and with the effects of input saturation are demonstrated to verify the effectiveness of the proposed controller in Section 4. And the conclusion is drawn in Section 5.

2. **Problem Statement and Preliminaries.**

2.1. **Kinematics and dynamics.**

In order to achieve good performance of DP control system, it is necessary to analyze kinematics and dynamics of DP ships. Two different reference coordinate systems including Earth-fixed frame O_E-$X_EY_EZ_E$ and body-fixed frame O_b-$X_bY_bZ_b$ (shown in Figure 1) are introduced to describe ship's kinematics. 3 degree-of-freedom (DOF) horizontal motion (surge, sway and yaw) of ship and low speed condition are usually researched in DP control system. Thus, the kinematics of DP ship is described as [1]:

$$\dot{\boldsymbol{\eta}} = \mathbf{R}(\psi)\boldsymbol{\upsilon} \tag{1}$$

where $\boldsymbol{\eta} = [x, y, \psi]^{\mathrm{T}} \in \Re^3$ is the vehicle's position and attitude vector in Earth-fixed frame. $\boldsymbol{\upsilon} = [u, v, r]^{\mathrm{T}} \in \Re^3$ represents the velocities in body-fixed frame. $\mathbf{R}(\psi) \in \Re^{3\times3}$ is transformation matrix between Earth-fixed frame and body-fixed frame with the properties of $\mathbf{R}^{-1}(\psi) = \mathbf{R}^{\mathrm{T}}(\psi)$, $\mathbf{R}(\psi)\mathbf{R}^{\mathrm{T}}(\psi) = I_{3\times3}$, $I_{n\times n}$ represents $n \times n$ identify matrix, and $\mathbf{R}(\psi)$ can be expressed by the following equation:

$$\mathbf{R}(\psi) = \begin{bmatrix} \cos(\psi) & -\sin(\psi) & 0 \\ \sin(\psi) & \cos(\psi) & 0 \\ 0 & 0 & 1 \end{bmatrix} \tag{2}$$

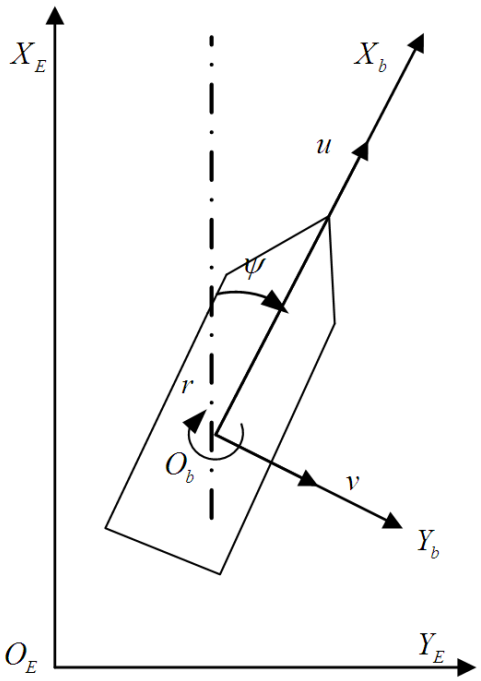

FIGURE 1. Two reference coordinate systems

Low frequency (LF) mathematical model of DP ship usually is used in DP control system. The LF model of ship [1] is described by

$$\mathbf{M}\dot{\boldsymbol{\upsilon}} + \mathbf{D}(\boldsymbol{\upsilon})\boldsymbol{\upsilon} + \mathbf{C}(\boldsymbol{\upsilon})\boldsymbol{\upsilon} = \boldsymbol{\tau}_c + \mathbf{R}^{\mathrm{T}}(\psi)\mathbf{b} \tag{3}$$

where $\mathbf{M} \in \Re^{3\times3}$, $\dot{\mathbf{M}} = \mathbf{0}$ is the total mass matrix containing the inertia mass matrix $\mathbf{M}_{RB} \in \Re^{3\times3}$, $\mathbf{M}_{RB} = \mathbf{M}_{RB}^{\mathrm{T}}$, $\dot{\mathbf{M}}_{RB} = \mathbf{0}$ and the added mass matrix $\mathbf{M}_A \in \Re^{3\times3}$ caused by the inertia of surrounding fluid; matrix of linearized damping forces and moments (neglecting heave, roll and pitch) $\mathbf{D}(\boldsymbol{\upsilon}) \in \Re^{3\times3}$ is usually positive definite matrix satisfying property of $\mathbf{D}(\boldsymbol{\upsilon}) = \mathbf{D}^{\mathrm{T}}(\boldsymbol{\upsilon})$; $\mathbf{C}(\boldsymbol{\upsilon}) \in \Re^{3\times3}$ is the matrix of Centripetal and Coriolis forces; $\mathbf{b} \in \Re^3$, $\mathbf{b} \leq B$ is bias vector containing slowly varying disturbances and unmodelled items; $\boldsymbol{\tau}_c \in \Re^3$ is control vector limited by thrusters' physical characteristics.

As for the DP control system, DP ship's kinematic and dynamic model (3) is transferred into

$$\mathbf{M}^*\ddot{\boldsymbol{\eta}} + \mathbf{D}^*\dot{\boldsymbol{\eta}} + \mathbf{C}^*\dot{\boldsymbol{\eta}} = \boldsymbol{\tau}_c^* + \mathbf{b}^* \tag{4}$$

where

$$\begin{aligned} &\mathbf{M}^* = \mathbf{R}(\boldsymbol{\psi})\mathbf{M}\mathbf{R}^{\mathrm{T}}(\boldsymbol{\psi}),\ \mathbf{D}^* = \mathbf{R}(\boldsymbol{\psi})\mathbf{D}(\boldsymbol{\upsilon})\mathbf{R}^{\mathrm{T}}(\boldsymbol{\psi}),\ \boldsymbol{\tau}_c^* = \mathbf{R}(\boldsymbol{\psi})\boldsymbol{\tau}_c, \\ &\mathbf{C}^* = \mathbf{R}(\boldsymbol{\psi})(\mathbf{C}(\boldsymbol{\upsilon}) - \mathbf{M}\mathbf{R}^{\mathrm{T}}(\boldsymbol{\psi})\dot{\mathbf{R}}(\boldsymbol{\psi}))\mathbf{R}^{\mathrm{T}}(\boldsymbol{\psi}),\ \mathbf{b}^* = \mathbf{R}(\boldsymbol{\psi})\mathbf{R}^{\mathrm{T}}(\boldsymbol{\psi})\mathbf{b} = \mathbf{b} \end{aligned} \tag{5}$$

In DP control system, slowly environmental disturbances $\mathbf{b}^*$ were derived in [19] and can be determined by formulas of environmental forces such as wind and 2-order wave forces.

2.2. **Control objective.** The desired position vector is defined as $\boldsymbol{\eta}_d = [\boldsymbol{\eta}_d(x), \boldsymbol{\eta}_d(y), \boldsymbol{\eta}_d(\psi)]^{\mathrm{T}}$. And desired position and attitude is assumed as $\boldsymbol{\eta}_{d0} = \begin{bmatrix} 20 & 10 & 5^\circ \end{bmatrix}^{\mathrm{T}}$. In order to generate smoothly desired path, the 2-order filter [8,19] is applied as

$$\begin{aligned} &\dot{\boldsymbol{\eta}}_d = \boldsymbol{\eta}_d \\ &\ddot{\boldsymbol{\eta}}_d = \omega_n^2\boldsymbol{\eta}_{d0} - \omega_n^2\boldsymbol{\eta}_d - \rho\,|\boldsymbol{\eta}_d|\,\boldsymbol{\eta}_d - 2\varsigma\omega_n\boldsymbol{\eta}_d \end{aligned} \tag{6}$$

where ω_n is the natural frequency, ς is the relative damping ratio, ρ is the designed parameter. Thus, the time histories of $\boldsymbol{\eta}_d$ in 3-DOF smoothly change to the desired values are shown in Figure 2. The desired trajectories as $\boldsymbol{\eta}_d(x), \boldsymbol{\eta}_d(y)$ and $\boldsymbol{\eta}_d(\psi)$ are smoothly and precisely approaching to the desired values from Figure 2 within 100s.

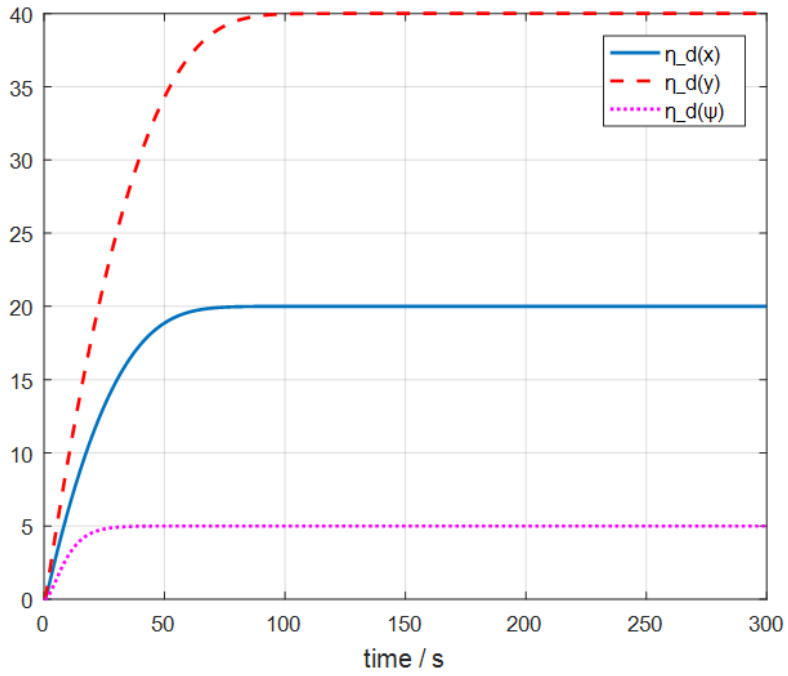

FIGURE 2. The time history of $\boldsymbol{\eta}_d$

The control objective is to design an SMC law $\boldsymbol{\tau}$ using RBF neural network to compensate input saturation and choose proper parameters so that the position $\boldsymbol{\eta}$ is accurately approached to the desired position $\boldsymbol{\eta}_d$ with disturbances and to maintain all input signals unifies asymptotic stability.

3. SMC Law Designed Using RBFNN.

This paper is to design SMC law $\boldsymbol{\tau}$ based on Laypunov stability theory utilizing RBFNN compensation to offset uncertainties in input forces and moment and reject environmental disturbances. And compare the designed control law to PID control law $\boldsymbol{\tau}_{PID}$ to clearly and intuitively demonstrate the effectiveness of the proposed control scheme.

3.1. Sliding mode controller designed.

SMC is a special nonlinear control strategy, and can steer the system motion along with desired trajectory. Define the error as $\mathbf{e} \in \Re^3$, that is

$$\mathbf{e} = \boldsymbol{\eta} - \boldsymbol{\eta}_d \tag{7}$$

Let $\dot{\boldsymbol{\eta}}_r = \dot{\boldsymbol{\eta}}_d - K_1\mathbf{e}, \boldsymbol{\upsilon}_r = \mathbf{R}^{\mathrm{T}}(\psi)\dot{\boldsymbol{\eta}}_r$ and the sliding mode function $\mathbf{s}$ is defined as

$$\begin{aligned} \mathbf{s} &= \dot{\boldsymbol{\eta}} - \dot{\boldsymbol{\eta}}_r = \dot{\mathbf{e}} + K_1\mathbf{e} \\ \dot{\boldsymbol{\eta}} &= \dot{\boldsymbol{\eta}}_r + \mathbf{s} \end{aligned} \tag{8}$$

where $K_1 \in \Re^{3\times3}$, $K_1 > 0^{3\times3}$ is gain matrix, which is constant value. Therefore,

$$\begin{aligned} \mathbf{M}^*\dot{\mathbf{s}} &= \mathbf{M}^*\left(\ddot{\boldsymbol{\eta}} - \ddot{\boldsymbol{\eta}}_r\right) \\ &= -\mathbf{M}^*\ddot{\boldsymbol{\eta}}_r - \left(\mathbf{C}^* + \mathbf{D}^*\right)\dot{\boldsymbol{\eta}} + \boldsymbol{\tau}_c^* + \mathbf{b}^* \\ &= -\mathbf{R}^{-\mathrm{T}}(\psi)\left(\mathbf{M}^*\dot{\boldsymbol{\upsilon}}_r - \left(\mathbf{C}^* + \mathbf{D}^*\right)\boldsymbol{\upsilon}_r\right) - \left(\mathbf{C}^* + \mathbf{D}^*\right)\mathbf{s} + \boldsymbol{\tau}_c^* + \mathbf{b}^* \end{aligned} \tag{9}$$

Thus, the common SMC law $\boldsymbol{\tau}_a$ is designed as

$$\boldsymbol{\tau}_a = \mathbf{R}^{-\mathrm{T}}(\psi)\left(\mathbf{M}^*\dot{\boldsymbol{\upsilon}}_r + \left(\mathbf{C}^* + \mathbf{D}^*\right)\boldsymbol{\upsilon}_r\right) - K_s\mathbf{s} - \mathbf{b}^* - K * \mathrm{sgn}(\mathbf{s}) \tag{10}$$

where $K_s = diag\{k_{s1}, k_{s2}, k_{s3}\}$, $K = diag\{d_1, d_2, d_3\}$ is the positive definite matrix.

For system (4), due to limitation of thrusters' physical characteristics, the control forces and moment are limited in a certain range. Assume that the maximum of control input is $\boldsymbol{\tau}_{c\max}$, define $\boldsymbol{\delta} = \boldsymbol{\tau}_c^* - \boldsymbol{\tau}_a$, $\boldsymbol{\tau}_c^* = sat(\boldsymbol{\tau})$. Thus, the control input limited function is

$$sat(\boldsymbol{\tau}) = \begin{cases} \boldsymbol{\tau}_{c\max}, & \boldsymbol{\tau}_a > \boldsymbol{\tau}_{c\max} \\ \boldsymbol{\tau}_a, & |\boldsymbol{\tau}_a| \le \boldsymbol{\tau}_{c\max} \\ -\boldsymbol{\tau}_{c\max}, & \boldsymbol{\tau}_a < -\boldsymbol{\tau}_{c\max} \end{cases} \tag{11}$$

The RBFNN input and output algorithm is chosen as

$$\begin{aligned} h_j &= \exp\left(\frac{\|x - c_j\|^2}{2b_j^2}\right) \\ \delta &= \{W_i^*\}^{\mathrm{T}} \bullet \{h_i(x)\} + \varepsilon \end{aligned} \tag{12}$$

where $x = \boldsymbol{\tau}_c^*$ is input of RBFNN, h_j, $j = 1, 2, \ldots, l$ is output vector of Gaussian radial basis functions, c_j represents the j-th neural centric position of hinder layer, b_j represents width of Gauss distribution, $\varepsilon \le \varepsilon_{\max}$ is the ideal neural network (NN) error approximating δ, the weight matrix is $W_i^* = \begin{bmatrix} W_{i1}^* & W_{i2}^* & \cdots & W_{il}^* \end{bmatrix}^{\mathrm{T}} \in \Re^l$, l is the number of product layer neurons, n is the dimensions of output and $i = 1, 2, \ldots, n$.

Therefore, there is assumption based on the approximation property of RBFNN, for any given $x \in \Omega$, Ω is compact set, and the optimal weight vector $\hat{W}_{op}$ is defined as

$$\hat{W}_{op} = \arg\min_{W^* \in \Omega_{W^*}} \left[\sup_{x \in \Omega} \left|\boldsymbol{\delta} - \hat{\boldsymbol{\delta}}\right|\right] \tag{13}$$

where $\Omega_{W^*} = \{W^* \,|\, \|W^*\| \le W_M^*\}$ is the feasible region of parameters, W_M^* is the designed parameters.

Define $\hat{\boldsymbol{\delta}}$ as output of NN, $\hat{W}^*$ as estimated weight, and thus the output of NN is

$$\hat{\boldsymbol{\delta}} = \hat{W}^{\mathrm{T}} h(x) \tag{14}$$

Let $\tilde{W} = \hat{W} - W^*$, thus

$$\boldsymbol{\delta} - \hat{\boldsymbol{\delta}} = W^{*\mathrm{T}} h(x) + \varepsilon - \hat{W}^{\mathrm{T}} h(x) = -\tilde{W}^{\mathrm{T}} h(x) + \varepsilon \tag{15}$$

Thus, the SMC law $\boldsymbol{\tau}_a$ with RBFNN is adjusted as

$$\boldsymbol{\tau}_a = \mathbf{R}^{-\mathrm{T}}(\psi)\left(\mathbf{M}^*\dot{\boldsymbol{\upsilon}}_r + \left(\mathbf{C}^* + \mathbf{D}^*\right)\boldsymbol{\upsilon}_r\right) - K_s\mathbf{s} - \mathbf{b}^* - K * \mathrm{sgn}(\mathbf{s}) - \hat{\boldsymbol{\delta}} \tag{16}$$

3.2. **Stability analysis.** For the above proposed control law of SMC with RBFNN for DP control system, it is necessary to verify the stability of the designed control law using Lyapunov stability theory.

Define Lyapunov function V as

$$V = \frac{1}{2}\mathbf{s}^{\mathrm{T}}\mathbf{M}^*\mathbf{s} + \frac{1}{2}\gamma\tilde{W}^{\mathrm{T}}\Gamma^{-1}\tilde{W} \tag{17}$$

where $\Gamma^{-1} \in \Re^{5\times5}$ is constant parameter matrix.

Therefore, the derivative of V is determined as

$$\begin{aligned} \dot{V} &= \mathbf{s}^{\mathrm{T}}\mathbf{M}^*\dot{\mathbf{s}} + \frac{1}{2}\mathbf{s}^{\mathrm{T}}\dot{\mathbf{M}}^*\mathbf{s} + tr\left(\tilde{W}^{\mathrm{T}}\Gamma^{-1}\dot{\tilde{W}}\right) \\ &= \mathbf{s}^{\mathrm{T}}\left(-\mathbf{R}^{-\mathrm{T}}(\psi)\left(\mathbf{M}^*\dot{\boldsymbol{\upsilon}}_r - \left(\mathbf{C}^* + \mathbf{D}^*\right)\boldsymbol{\upsilon}_r\right) - \left(\mathbf{C}^* + \mathbf{D}^*\right)\mathbf{s} + \boldsymbol{\tau}_c^* + \mathbf{b}^*\right) \\ &\quad + \frac{1}{2}\mathbf{s}^{\mathrm{T}}\dot{\mathbf{M}}^*\mathbf{s} + tr\left(\tilde{W}^{\mathrm{T}}\Gamma^{-1}\dot{\tilde{W}}\right) \end{aligned} \tag{18}$$

$$= -\mathbf{s}^{\mathrm{T}}\left(\mathbf{C}^{*}+\mathbf{D}^{*}\right)\mathbf{s}-\mathbf{s}^{\mathrm{T}}\left(\mathbf{R}^{-\mathrm{T}}(\psi)\left(\mathbf{M}^{*}\dot{\boldsymbol{\upsilon}}_{r}+\left(\mathbf{C}^{*}+\mathbf{D}^{*}\right)\boldsymbol{\upsilon}_{r}\right)\right)+\mathbf{s}^{\mathrm{T}}\mathbf{b}^{*}+\mathbf{s}^{\mathrm{T}}\boldsymbol{\tau}_{a}$$
$$+\frac{1}{2}\mathbf{s}^{\mathrm{T}}\dot{\mathbf{M}}^{*}\mathbf{s}+tr\left(\tilde{W}^{\mathrm{T}}\Gamma^{-1}\dot{\tilde{W}}\right)$$

Due to $\mathbf{s}^{\mathrm{T}}\dot{\mathbf{M}}^{*}\mathbf{s}=0$, $\mathbf{s}^{\mathrm{T}}\mathbf{C}^{*}\mathbf{s}=0$, combining with (16), $\dot{V}$ is derived as

$$\begin{aligned}\dot{V} =& -\mathbf{s}^{\mathrm{T}}\left(\mathbf{C}^{*}+\mathbf{D}^{*}\right)\mathbf{s}-\mathbf{s}^{\mathrm{T}}\left(\mathbf{R}^{-\mathrm{T}}\left(\psi\right)\left(\mathbf{M}^{*}\dot{\boldsymbol{\upsilon}}_{r}+\left(\mathbf{C}^{*}+\mathbf{D}^{*}\right)\boldsymbol{\upsilon}_{r}\right)\right)+\mathbf{s}^{\mathrm{T}}\mathbf{b}^{*}\\ &+\mathbf{s}^{\mathrm{T}}\left(\mathbf{R}^{-\mathrm{T}}(\psi)\left(\mathbf{M}^{*}\dot{\boldsymbol{\upsilon}}_{r}+\left(\mathbf{C}^{*}+\mathbf{D}^{*}\right)\boldsymbol{\upsilon}_{r}\right)-K_{s}\mathbf{s}-\mathbf{b}^{*}-K*\operatorname{sgn}(\mathbf{s})-\hat{\boldsymbol{\delta}}\right)\\ &+\frac{1}{2}\mathbf{s}^{\mathrm{T}}\dot{\mathbf{M}}^{*}\mathbf{s}+tr\left(\tilde{W}^{\mathrm{T}}\Gamma^{-1}\dot{\tilde{W}}\right)\\ =& -\mathbf{s}^{\mathrm{T}}\left(\mathbf{C}^{*}+\mathbf{D}^{*}\right)\mathbf{s}-\mathbf{s}^{\mathrm{T}}K_{d}\mathbf{s}-\mathbf{s}^{\mathrm{T}}K*\operatorname{sgn}(\mathbf{s})+\frac{1}{2}\mathbf{s}^{\mathrm{T}}\dot{\mathbf{M}}^{*}\mathbf{s}+tr\left(\tilde{W}^{\mathrm{T}}\Gamma^{-1}\dot{\tilde{W}}\right)\\ =& -\mathbf{s}^{\mathrm{T}}K_{s}\mathbf{s}-K\|\mathbf{s}\|+\tilde{W}^{\mathrm{T}}\left(\Gamma^{-1}\dot{\tilde{W}}-h(x)\mathbf{s}^{\mathrm{T}}\right)\end{aligned} \tag{19}$$

Therefore, the adaptive neural network law $\dot{\tilde{W}}$ is

$$\dot{\tilde{W}}=\Gamma^{-1}h(x)\mathbf{s}^{\mathrm{T}} \tag{20}$$

Thus, the $\dot{V}$ is determined as

$$\dot{V}=-\mathbf{s}^{\mathrm{T}}K_{d}\mathbf{s}-K\|\mathbf{s}\|+\sum_{i=1}^{n}\left(\tilde{W}_{i}^{\mathrm{T}}\Gamma^{-1}\dot{\tilde{W}}-\tilde{W}_{i}^{\mathrm{T}}h(x)\right)=-\mathbf{s}^{\mathrm{T}}K_{d}\mathbf{s}-K\|\mathbf{s}\|\leq 0 \tag{21}$$

Consequently, the system is stable based on Lyapunov stabilization theories.

3.3. **PID control law designed.** In order to demonstrate advantages and disadvantages of the above proposed control law τ_a, PID conventional control law is introduced in this part to compare to the designed control law. Thus, the differences between PID control law and proposed control law are more clear and intuitive.

Define the position and velocity errors as $\mathbf{e}=\boldsymbol{\eta}_{PID}-\boldsymbol{\eta}_{d}$, $\dot{\mathbf{e}}=\dot{\boldsymbol{\eta}}_{PID}-\dot{\boldsymbol{\eta}}_{d}$, and the PID control law $\boldsymbol{\tau}_{PID}$ is derived as [1]

$$\boldsymbol{\tau}_{PID}=K_{P}\mathbf{e}+K_{I}\int_{0}^{t}\mathbf{e}dt+K_{D}\dot{\mathbf{e}} \tag{22}$$

where K_P, K_I, $K_D\in\Re^{3\times 3}$ are the control gain matrices and are selected as positive diagonal matrix.

4. **Simulation Results.** This section is including the ship and control parameters and the simulation results of Section 3.

4.1. **Ship and control parameters.** In order to verify the effectiveness of the proposed control scheme, ship and control parameters are necessary to be given before simulation. To derive environmental disturbances, parameters are given as wind speed is 20 m/s, wind direction is 30° and wave direction is 30°.

For ship model, assume that the initial value of matrix $\mathbf{C}$ is zero and ship parameters introduced in Section 2.1 are listed as

$$\begin{aligned}\mathbf{M}&=\begin{bmatrix}9.1948\times10^{7} & 0 & 0\\ 0 & 9.1948\times10^{7} & 9.6979\times10^{8}\\ 0 & 9.6979\times10^{8} & 1.0724\times10^{11}\end{bmatrix}\\ \mathbf{D}&=\begin{bmatrix}1.5073\times10^{6} & 0 & 0\\ 0 & 8.1687\times10^{6} & 9.6979\times10^{8}\\ 0 & 9.6979\times10^{8} & 1.2568\times10^{11}\end{bmatrix}\end{aligned} \tag{23}$$

The initial values of ship position and initial velocity are zero. The value of $\boldsymbol{\tau}_{c\max}$ is

$$\boldsymbol{\tau}_{c\max} = \left[\begin{array}{ccc} 3.2e+6 & 2e+6 & 1.7e+8 \end{array} \right]^{\mathrm{T}} \tag{24}$$

Gain matrices for K_1, K_d, K introduced in Section 3.1 are chosen as

$$K_1 = diag\left\{1, 1, 1\right\}, \quad K_d = diag\left\{1e5, 5e6, 8e9\right\}, \quad K = diag\left\{1e5, 1e5, 1e5\right\} \tag{25}$$

And the gain matrices of conventional PID control law mentioned in Section 3.3 are selected as

$$\begin{gathered} K_p = -diag\left\{4e5, 1e7, 5e8\right\}, \quad K_i = -diag\left\{1e1, 0e2, 1e1\right\}, \\ K_d = -diag\left\{5e7, 5e8, 4e10\right\} \end{gathered} \tag{26}$$

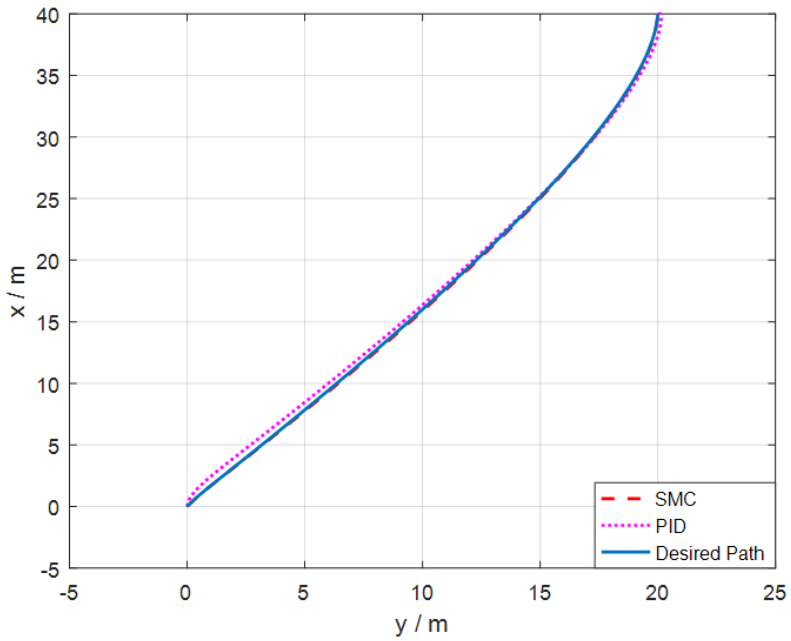

FIGURE 3. Time history of ship motion without input saturation

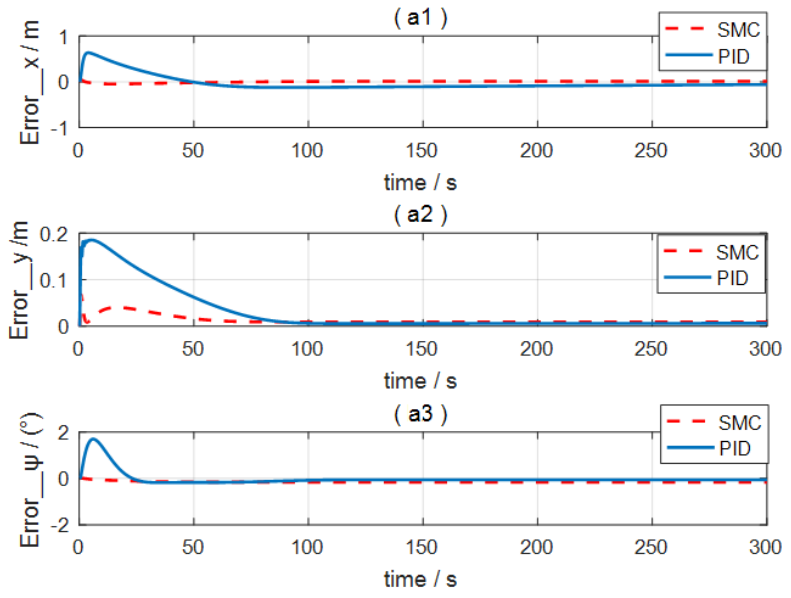

FIGURE 4. Position and attitude errors without input saturation

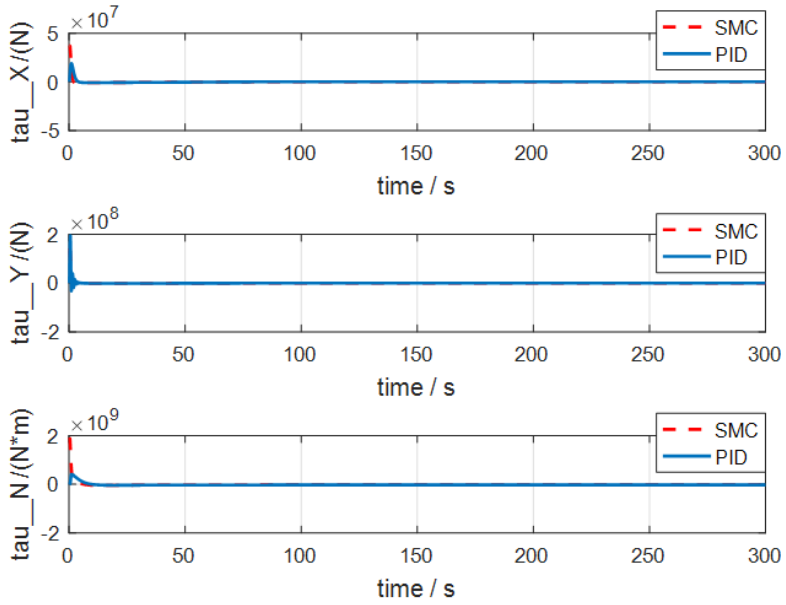

FIGURE 5. Control forces and moment without input saturation

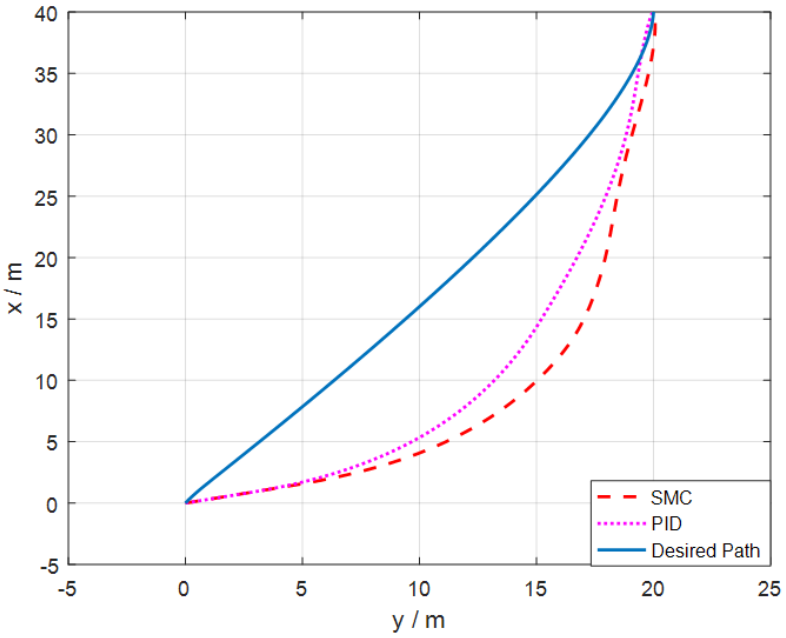

FIGURE 6. Time history of ship motion with input saturation

4.2. **Analysis and discussion for simulation results.** Simulation results for DP control system are represented in three groups: firstly, simulation results without input saturation under control of the proposed SMC law and PID control law are shown in Figure 3, Figure 4, Figure 5; secondly, simulation results with input saturation under the SMC law and PID control law are shown in Figure 6, Figure 7, Figure 8; thirdly, simulation results of the designed SMC law with RBFNN compared to PID control law with input saturation are shown in Figure 9, Figure 10 and Figure 11. The three groups of figures are demonstrated in three aspects, that is, time history of ship motion, errors in surge, sway and yaw directions and the control forces and moment to compare the designed control law to PID control law.

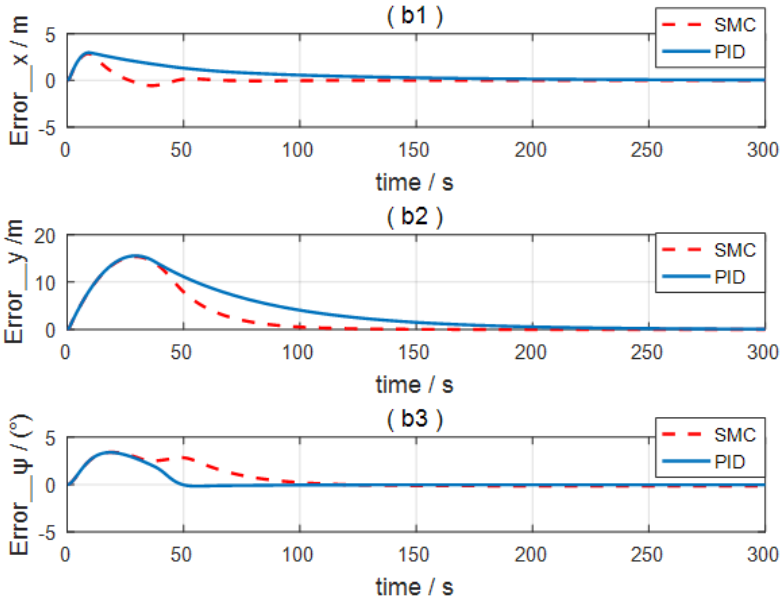

FIGURE 7. Position and attitude error with input saturation

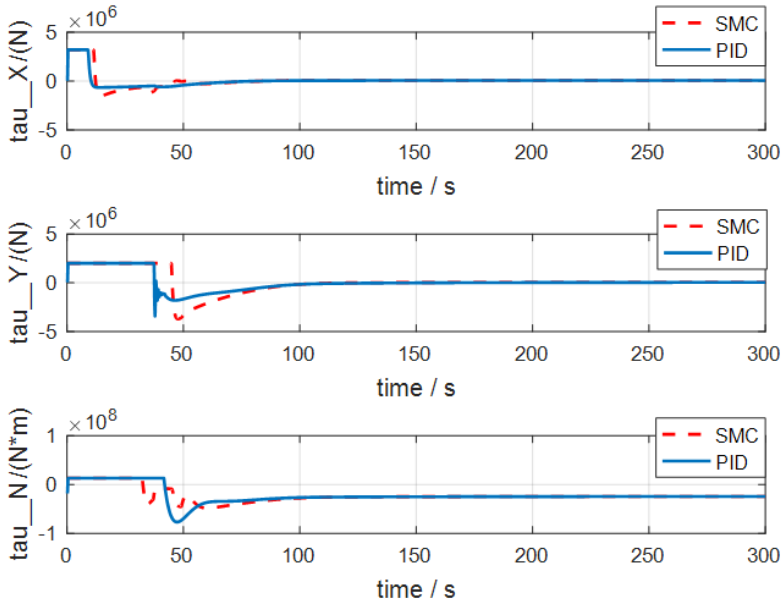

FIGURE 8. Control forces and moment with input saturation

Simulation results without input saturation are shown in Figure 3, Figure 4, Figure 5. And both designed SMC law and PID law can steer the ships precisely move to desired position and the motion path is very smooth in Figure 3. In addition, Figure 4(a1) shows that the errors in surge within 0.25m under SMC law preferred than PID control law within 0.5m. Similarly, Figure 4(a2) indicates the largest errors in sway within 0.1m under SMC law and the largest error within 0.2m. Especially, in Figure 4(a3), the largest errors in yaw directions under designed SMC law are also smaller than PID control law in condition of without input saturation. Thus, the SMC law is in greater stability with smaller errors in three directions. And Figure 5 indicates the output maximum of control forces and moment exceeded to the thrusters' maximum values in three directions, though errors of position and attitude are very small under the two control methods. Therefore,

the output of control forces and moment under SMC are very dangerous in real DP control operation.

After considering the problem of input saturation, the time history of motion is shown in Figure 6, though both PID control law and SMC law are worse than without input saturation, the two control laws can steer ships move to the desired position. From Figure 7(b1), the rising time in surge direction is about 50s under SMC law instead of 100s under PID control law; similarly, the rising time in sway direction under SMC law is shorter 100s than PID control law in Figure 7(b2); but there is a larger overshoot in yaw direction under SMC law within 100s in Figure 7(b3). In Figure 8, the control forces and moment

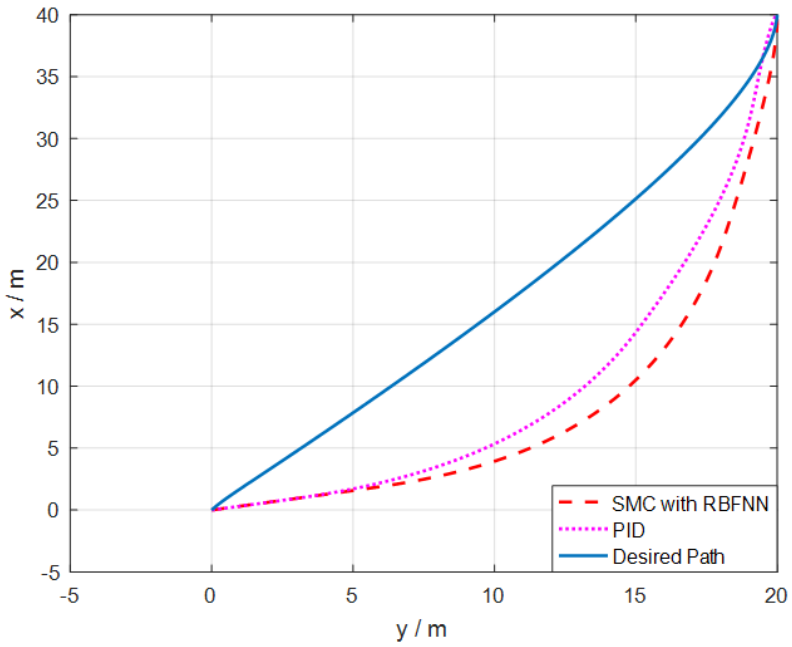

FIGURE 9. Time history of ship motion with input saturation

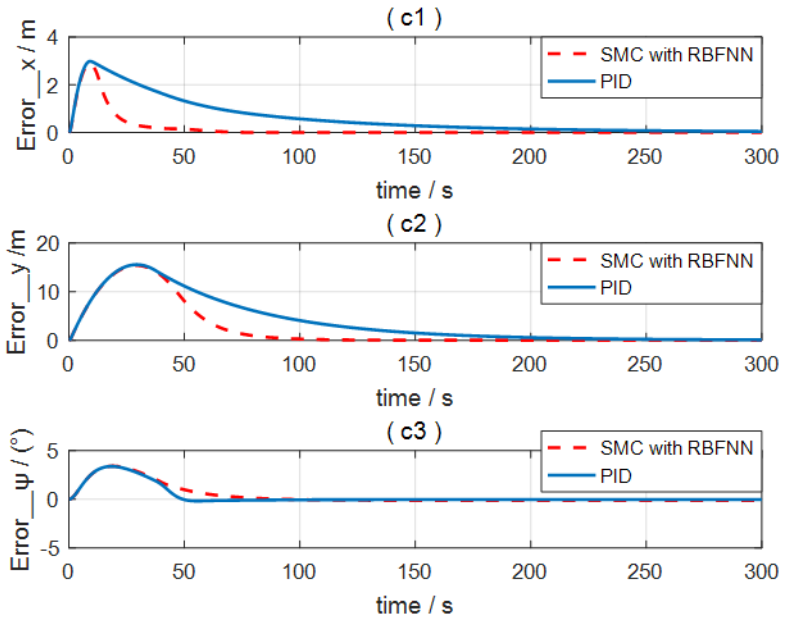

FIGURE 10. Position and attitude error with input saturation

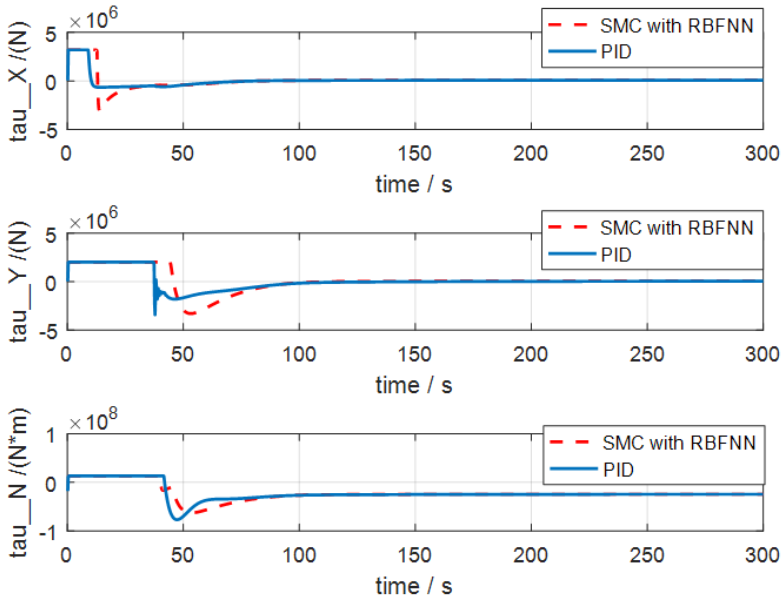

FIGURE 11. Control forces and moment with input saturation

in 3-DOF do not exceed the maximum values under the limitation of input saturation both in SMC law and PID control law. After adding the RBFNN compensation, the simulation results of SMC law are shown in Figure 9, Figure 10 and Figure 11. Time history of motion shown in Figure 9 indicates that both SMC law with RBFNN and PID control law can steer ships move to the desired position. From Figure 10(c1), the rising time in surge direction under SMC law with RBFNN is shorter 130s than PID control law; similarly, the rising time in sway direction under SMC law with RBFNN is shorter 120s than PID control law in Figure 10(c2); and the overshoot in yaw direction is less under SMC law with RBFNN in Figure 10(c3). In Figure 11, the control forces and moment in three directions are limited within the maximum values and are more smooth under SMC law with RBFNN compensation than PID control law.

5. **Conclusions.** In this paper, the problems in DP ship control for offshore structures with disturbances and input saturation have been researched under SMC with RBFNN compensation. After adding input saturation, the values of forces and moment are smaller than without input limitation, though the errors of the designed SMC law with RBFNN compensation are larger, the rising times in surge and sway directions are shorter compared to PID control law. And the chattering phenomenon occurs in forces and moment curves. Thus, the new problem about the SMC law chattering is emerged to affect the control performance. Therefore, the chatting problem of SMC is the future research thing and needs to solve in future.

Acknowledgment. This work was supported by the National Natural Science Foundation of China (No. 51609046), and the Fundamental Research Funds for the Central Universities (HEUCFM170403).

REFERENCES

[1] A. J. Sørensen, A survey of dynamic positioning control systems, *Annual Reviews in Control*, vol.35, no.1, pp.123-136, 2011.

[2] L. Xu and Z. Q. Liu, Design of fuzzy PID controller for ship dynamic positioning, *Chinese Control and Decision Conference*, Yinchuan, China, pp.3130-3135, 2016.

[3] X. Hu, J. Du and J. Shi, Adaptive fuzzy controller design for dynamic positioning system of vessels, *Applied Ocean Research*, vol.53, pp.46-53, 2015.
[4] J. Du, X. Hu, M. Krstić and Y. Sun, Robust dynamic positioning of ships with disturbances under input saturation, *Automatica*, vol.73, pp.207-214, 2016.
[5] O. M. R. Rabanal, A. H. Brodtkorb and M. Breivik, Comparing controllers for dynamic positioning of ships in extreme seas, *IFAC Papers Online*, vol.49, no.23, pp.258-264, 2016.
[6] J. Du, X. Hu, H. Liu and C. L. Chen, Adaptive robust output feedback control for a marine dynamic positioning system based on a high-gain observer, *IEEE Trans. Neural Networks & Learning Systems*, vol.26, no.11, pp.2775-2786, 2015.
[7] A. Veksler, T. A. Johansen, F. Borrelli and B. Realfsen, Dynamic positioning with model predictive control, *IEEE Trans. Control Systems Technology*, vol.24, no.4, pp.1340-1353, 2016.
[8] G. Xia, J. Xue, J. Jiao et al., Adaptive fuzzy control for dynamic positioning ships with time-delay of actuator, *IEEE/MTS Oceans*, Monterey, USA, pp.1-6, 2016.
[9] A. Nasiri, S. K. Nguang and A. Swain, Adaptive sliding mode control for a class of MIMO nonlinear systems with uncertainties, *Journal of the Franklin Institute*, vol.351, no.4, pp.2048-2061, 2014.
[10] J. Zhu and K. Khayati, On a new adaptive sliding mode control for MIMO nonlinear systems with uncertainties of unknown bounds, *International Journal of Robust & Nonlinear Control*, vol.27, pp.942-962, 2017.
[11] P. Li, J. Ma and Z. Zheng, Robust adaptive sliding mode control for uncertain nonlinear MIMO system with guaranteed steady state tracking error bounds, *Journal of the Franklin Institute*, vol.353, no.2, pp.303-321, 2016.
[12] M. Chen, S. Chen and Q. Wu, Sliding mode disturbance observer-based adaptive control for uncertain MIMO nonlinear systems with deadzone, *International Journal of Adaptive Control and Signal Processing*, vol.31, no.7, pp.1003-1018, 2017.
[13] G. Xia, C. Pang and J. Xue, Fuzzy neural network-based robust adaptive control for dynamic positioning of underwater vehicles with input dead-zone, *Journal of Intelligent & Fuzzy Systems*, vol.29, no.6, pp.2585-2595, 2015.
[14] M. C. Pai, Dynamic output feedback RBF neural network sliding mode control for robust tracking and model following, *Nonlinear Dynamics*, vol.79, no.2, pp.1023-1033, 2015.
[15] M. Zhang, X. Shen and T. Li, Fault tolerant attitude control for cubesats with input saturation based on dynamic adaptive neural network, *International Journal of Innovative Computing, Information and Control*, vol.12, no.2, pp.651-663, 2016.
[16] Z. Zheng and L. Sun, Path following control for marine surface vessel with uncertainties and input saturation, *Neurocomputing*, vol.177, pp.158-167, 2016.
[17] D. Mu, G. Wang, Y. Fan and Y. Zhao, Design of robust adaptive course controller for unmanned surface vehicle with input saturation, *International Journal of Innovative Computing, Information and Control*, vol.13, no.5, pp.1751-1758, 2017.
[18] J. Huang, C. Wen, W. Wang et al., Global stable tracking control of underactuated ships with input saturation, *Systems & Control Letters*, vol.85, pp.1-7, 2015.
[19] G. Xia, J. Xue and J. Jiao, Dynamic positioning control system with input time-delay using fuzzy approximation approach, *International Journal of Fuzzy Systems*, vol.20, no.2, pp.630-639, 2018.